

Single crystal diamond tips for scanning probe microscopy

Alexander N. Obraztsov, Petr G. Kopylov, Boris A. Loginov, Mathew A. Dolganov, Rinat R. Ismagilov et al.

Citation: *Rev. Sci. Instrum.* **81**, 013703 (2010); doi: 10.1063/1.3280182

View online: <http://dx.doi.org/10.1063/1.3280182>

View Table of Contents: <http://rsi.aip.org/resource/1/RSINAK/v81/i1>

Published by the [American Institute of Physics](#).

Additional information on *Rev. Sci. Instrum.*

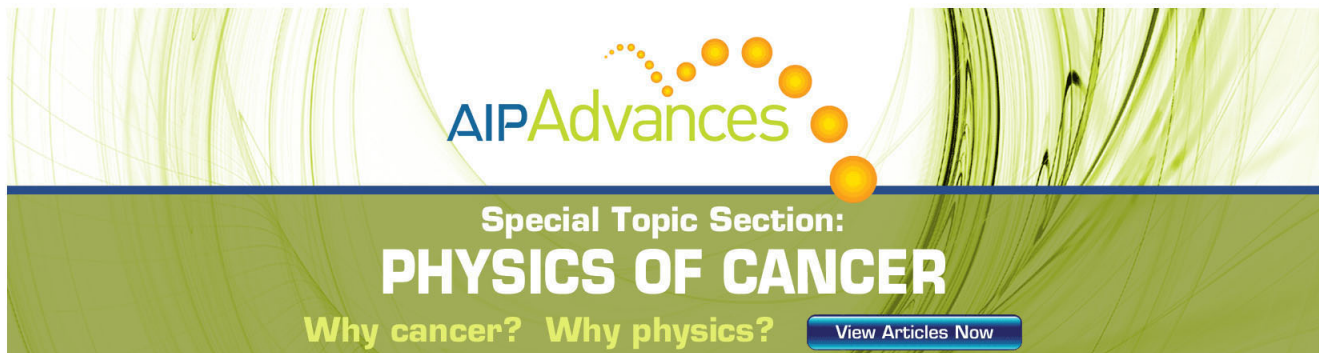
Journal Homepage: <http://rsi.aip.org>

Journal Information: http://rsi.aip.org/about/about_the_journal

Top downloads: http://rsi.aip.org/features/most_downloaded

Information for Authors: <http://rsi.aip.org/authors>

ADVERTISEMENT



AIP Advances

Special Topic Section:
PHYSICS OF CANCER

Why cancer? Why physics? [View Articles Now](#)

Single crystal diamond tips for scanning probe microscopy

Alexander N. Obraztsov,^{1,2,a)} Petr G. Kopylov,¹ Boris A. Loginov,³ Mathew A. Dolganov,¹ Rinat R. Ismagilov,^{1,2} and Natalia V. Savenko⁴

¹*Department of Physics, Moscow State University, Moscow 119991, Russia*

²*Department of Physics and Mathematics, University of Joensuu, Joensuu 80101, Finland*

³*Moscow Institute of Electronic Technology, Moscow 124498, Russia*

⁴*Estonian Nanotechnology Competence Centre, Tartu 51014, Estonia*

(Received 29 October 2009; accepted 8 December 2009; published online 14 January 2010)

Single crystal diamond tips with perfect pyramidal geometry were obtained by a combination of chemical vapor deposition and selective oxidation of polycrystalline films. The parameters of the deposition process were chosen to provide growth of a textured film consisting of micrometer sized diamond crystallites embedded into nanodiamond ballas-like material. The heating of the film in an air environment was used for selective oxidation of the nanodiamond component. The films obtained contain free standing pyramidal single crystal diamond tips oriented by their apexes to the substrate surface. The tips were used for the fabrication of atomic force microscopy probes and their evaluation in comparison to common silicon probes. © 2010 American Institute of Physics.

[doi:10.1063/1.3280182]

I. INTRODUCTION

Exceptional mechanical, thermal, optical, and electronic properties make diamond very attractive for numerous applications. However, exploitation of these advantages is hampered by difficulties in obtaining the desired geometry of diamond. In particular, tip-shaped diamonds are desired for different types of scanning probe microscopes,^{1–3} indenters,⁴ nanolithography,^{5,6} and other similar applications (see e.g. Refs. 7–9). To obtain diamond tips, it has been proposed to use micromachining of single crystals,¹ plasma,^{10,11} or reactive ion¹² etching of polycrystalline diamond films, and chemical vapor deposition (CVD) growth on tip-shaped^{13,14} or pyramidal pit etched substrates.^{6,15} These technologies are able to provide advantageous results. For example, the AFM probes produced from nanocrystalline CVD diamond have been found to be nearly ten times more wear resistant than commercially available silicon nitride probes.¹⁵ However, most of these methods provide tips with polycrystalline or highly defective apexes having rather large radii of curvature. The micromachined single crystal diamond tips are very difficult and expensive to fabricate with reproducible geometric characteristics, crystallographic orientation, and other properties. In this paper, we present a new method allowing for mass production of single crystal micrometer-sized diamond tips having perfect pyramidal shapes and a radius of curvature at their apex in the range of a few nanometers.

II. EXPERIMENTAL METHOD

The proposed method is based on well known facts about diamond crystal growth and oxidation (e.g., see Refs. 16–18). One of the essential features of the CVD process is directional growth of diamond crystallites. Starting from ini-

tial nuclei of nanometer size, the dimensions of growing crystallites increase with deposition time. But at some stage of the process, only upper surfaces (with respect to the direction perpendicular to the substrate surface) may receive enough feeding by the carbonaceous precursors, while other lateral surfaces are shielded from the gas phase by the neighboring crystallites. This results in a columnar structure of the CVD polycrystalline films. The crystallographic orientations of the crystallites are determined by the ratio of the growth rates for different directions which may be controlled by the CVD process parameters. It is important to note that the fastest growth rates correspond to the most defective facets. For diamond, this is (111) and (110) directions, while the lowest growth rate is for the (100) direction, providing the highest level of crystal ordering for the {100} growth sectors. The density of structural defects determines the chemical stability of the facets and thus {100} facets must be much more resistant to oxidation compared to {110} and, especially, {111} diamond crystal facets. The oxidation rate is also drastically increased and the oxidation temperature is reduced down to about 600 °C with a decrease of the diamond crystallite sizes to nanometer range.^{19,20} This is because a significant amount of the total number of atoms in the nanosized diamond is located on the surface and thus belongs to a structurally defective and thermodynamically unstable region.²¹

In the present work, the synthesis of the diamond films was performed using a CVD system described in detail in Ref. 22. The deposition occurs from a hydrogen-methane gas mixture activated by a direct current (dc) discharge. The deposition parameters were chosen in such a manner as to provide a mixture of nanodiamond material with inclusions of well developed microcrystalline diamonds: the substrate temperature was about 900 °C; gas mixture composition of CH₄:H₂=5:95; total gas pressure of 9.5 kPa; dc discharge voltage of 750 V and current density of 0.7 A/cm²; duration

^{a)} Author to whom correspondence should be addressed. Electronic mail: obraz@polly.phys.msu.ru.

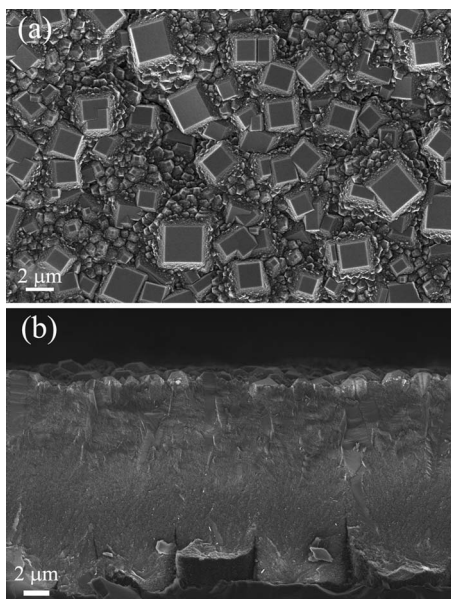


FIG. 1. SEM images of the surface (a) and a cross-section (b) of the CVD diamond film grown under conditions providing rectangular (100) facets on the film surface.

of the deposition process - 180 min. Standard silicon wafers [Si (100), 460 μm thickness] were used as substrates. Before being used for diamond deposition, the substrates were treated with micrometer sized diamond powder to increase the density of nucleation sites. The treatments were made either by mechanical scratching or by ultrasonication in an aqueous suspension of the diamond powder, both methods resulting in similar characteristics for the obtained CVD diamond films (see details in Ref. 22).

III. RESULTS AND DISCUSSION

Figure 1 shows typical scanning electron microscopy (SEM) images of the CVD films obtained at the above mentioned conditions. The films consist of a mixture of micrometer sized crystallites, having well developed rectangular (100) facets on the film surface, and submicrometer and nanometer sized species with shapes which cannot be resolved by the SEM [Fig. 1(a)]. A cross-sectional view [Fig. 1(b)] shows that the main part of the film has a homogeneously dense structure, except for the interface region near the substrate.

Raman spectroscopy analysis (see Fig. 2, curve 1) reveals that the films consist of diamond crystallites of different sizes, graphitic inclusions, and amorphous carbon: the line centered at about 1332 cm^{-1} corresponds to micrometer sized diamond; lines at 1140 and 1470 cm^{-1} are assigned to nanometer sized crystallites; lines at 1350 and 1580 cm^{-1} relate to crystalline graphite and amorphous carbon.^{17,18}

The CVD films of this type were oxidized by exposure to normal air atmosphere at a temperature of 650 $^{\circ}\text{C}$ for 10 h. Figure 3 shows SEM images obtained for the oxidized CVD film. It is clearly seen from Fig. 3(a) that only the fraction of the crystallites with the largest dimension is present in the film after oxidation. These crystallites have rectangular facets on their tops. The lateral facets of the crys-

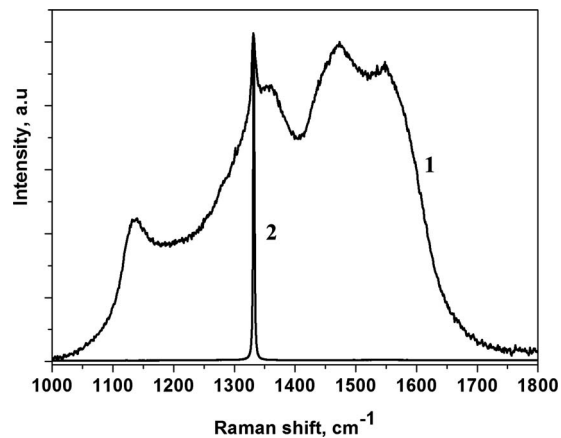


FIG. 2. Typical Raman spectra for as-grown CVD film (curve 1) and for the same film after oxidation (curve 2). The spectra are normalized to the intensity of the Raman line centered at about 1332 cm^{-1} corresponding to diamond.

tallites are evident from Fig. 3(b) obtained for the same sample after slight mechanical pressing by tweezers. These lateral facets have a triangular shape and form diamond crystallites with a rather perfect pyramidal geometry. In the as grown films, these pyramids are oriented by their apexes to the substrate surface. As a result of the oxidation, the connection of the pyramidal diamond crystallites to the surface weakens and even a very gentle mechanical press can push them over.

The Raman spectrum of the oxidized CVD film demonstrates a strong “diamond” line at about 1332 cm^{-1} only. The line width is reduced from about 8 cm^{-1} for the as grown film to 2.5 cm^{-1} for the oxidized material which corresponds to single crystal diamond.^{17,18} Together with an absence of the “nanodiamond” and “graphitic” lines in the Raman spectrum of the oxidized diamond film, this proves that oxidation removes the most defective and nondiamond parts of the

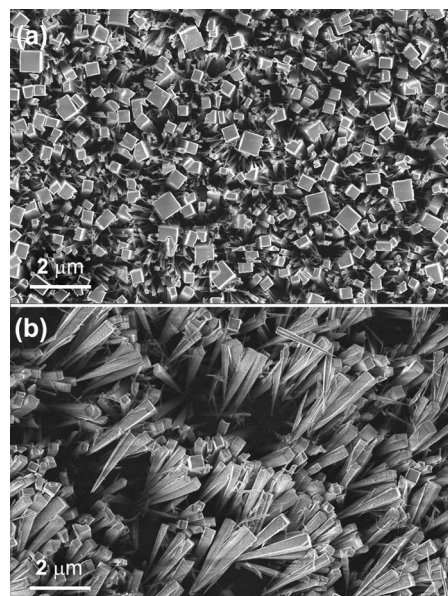


FIG. 3. SEM images of the CVD diamond film surface after oxidation with diamond single crystal pyramids in their original orientation (a) and fallen after gentle touching of the surface by tweezers (b).

CVD film. In the as grown film, these fractions fill out space between the pyramidal core crystallites. The sizes of the diamond single crystal pyramids obtained at the described condition are about 10–15 μm in length and have about 4–5 μm edges of the rectangular base plane. These planes are practically squares that correspond to the $\{100\}$ diamond facet. Oxidation does not produce any significant changes in the shape and flatness of these base planes. The apexes of the pyramids have a typical radius of curvature in the range of 20–2 nm. The last number corresponds to the smallest size of thermodynamically stable diamond.²¹

While the described results are properly consistent to known principles of CVD diamond growth and oxidation (see above), for the first time, we were able to produce micrometer sized single diamond crystallites of perfect pyramidal shape. The use of CVD technology allows for very easy and inexpensive mass production of this type of diamond tips which may be attractive for different applications. In this work, atomic force microscopy (AFM) probes were manufactured by attaching the diamond tips to standard (silicon and silicon-nitride) cantilevers. Figure 4(a) shows a SEM image of the AFM probe with a diamond tip glued to a silicon cantilever (supplied by Mikromasch Com.) by an epoxy. Similar diamond AFM probes were tested with different samples. Figures 4(b) and 4(c) show the comparative test made using a sample of a TiN film deposited onto polished ($R_a < 10$ nm) glass by magnetron sputtering. The TiN film thickness was about 200 nm.

The tests were performed in contact mode using atomic force microscope SMM-2000 (PROTON-MIET Co., Russia). The diamond tips were glued to “soft” cantilevers MSCT-AUHV type “C” (Veeco, USA). The stiffness of the cantilevers used was 0.01 N/m and an applied force was of about 10^{-12} N, corresponding to a bending of the end of the cantilever about 100 pm. To estimate profile resolution, the additional test measurements were performed with the diamond probes for the fresh cleavages of mica. We were able to obtain atomic resolution for the mica samples with used AFM device and with diamond tips having radius of curvature at apex in range of 2.5–10 nm. This allows us to estimate an accuracy of the profile measurements to be better than 0.002 nm for 5 nm tips and even more for the tips with smaller radius. This accuracy for the profile measurements may be realized in the conditions of soft contact mode provided by used AFM device and cantilevers. At the same time, a lateral resolution depends only on the probe apex curvature which is the most interesting parameter of the diamond tips to be tested. The comparative data were obtained using standard silicon probes on the same type cantilever MSCT-AUHV type C (Veeco, USA).

In the test measurements, scanning of the TiN surface was performed by gradually increasing the lateral resolution up to the moment when the resulting AFM images became blurred. The resolution increase was obtained by reducing size of the scanned area with the same number 500×500 points in the scans, and the image blurring corresponds to the situation when the neighboring points in the scan have identical parameters. An example of such a blurred image obtained using a standard Si probe is shown in Fig.

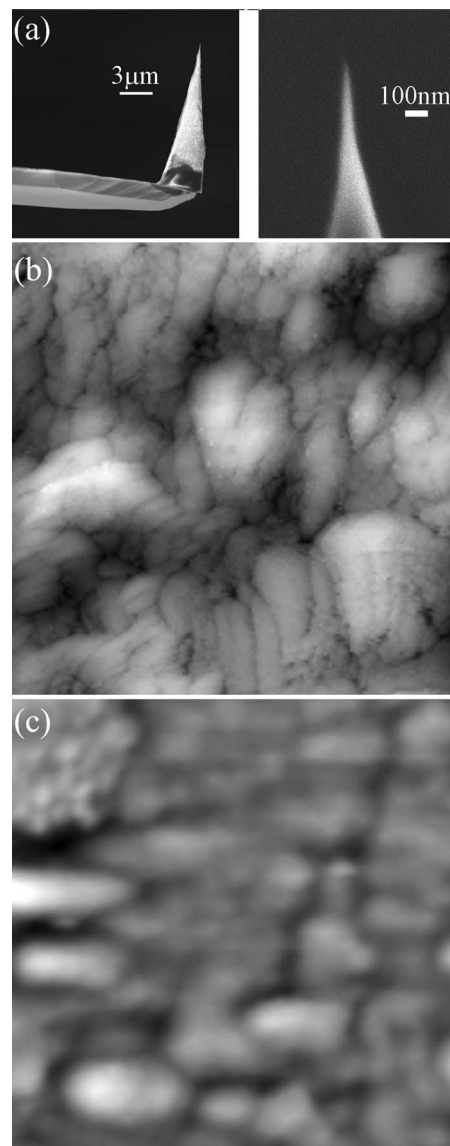


FIG. 4. SEM image of an AFM probe made by gluing a single crystal diamond tip to a silicon cantilever (a). AFM images obtained for the TiN film sample using the diamond probe (b) and the common silicon probe (c). The size of the AFM scans is 300×300 nm².

4(c). Figure 4(b) shows the AFM image obtained under the same conditions, but using the diamond tip probe. The improvement of AFM imaging with the use of the diamond probe is evident. Moreover, usage of the diamond tip allows even better resolution than that demonstrated in Fig. 4(b). This visual comparison of sharpness of the AFM images allows us to estimate that the resolution of the diamond probes is 50 times better in comparison with used silicon tip.

Other advantages of the diamond probes were found in the test measurements made for the biological objects. Due to the hydrophobicity of the surface, the diamond probes show a much better efficiency (higher resolution combined with much longer life time) in comparison with typical silicon probes. The chemical inertness of diamond is an important factor providing better imaging performance of the diamond AFM probes. The excellent wear resistance of diamond can play a significant role in other applications including, for example, dip pen nanolithography,²⁵ probe based

nanopatterning,²⁴ atomic force acoustic microscopy,²⁵ etc. The diamond tips with low wear rates can prove useful because the features sizes and data interpretation in these applications depend on the tip radius and may change due to tip wear.

IV. CONCLUSION

In this work, we demonstrated the ability to produce single crystal diamonds of micrometer size with regular pyramidal shape having a square base plane and a tiny pointed apex. The developed methods, based on CVD film growth and selective oxidation, provide inexpensive mass production of the diamond pyramidal tips suitable for different applications. In particular, we demonstrated the possibility for efficient application of the diamond tips as AFM probes.

ACKNOWLEDGMENTS

This work was supported by the Russian Foundation for Basic Researches (Grant No. 09-01-12024 ofi-m), the Academy of Finland (Grant Nos. 123252 and 124133) and by the European Community's ERDF 3.1.9 funding (Grant No. EU28609).

¹B. Mesa and S. Magonov, *J. of Physics: Conf. Ser.* **61**, 770 (2007).

²M. R. Jarvis, R. Perez, and M. C. Payne, *Phys. Rev. Lett.* **86**, 1287 (2001).

³T. Hantschel, P. Niedermann, T. Trenkler, and W. Vandervorst, *Appl. Phys. Lett.* **76**, 1603 (2000).

⁴B. Bhushan and V. N. Koinkar, *Appl. Phys. Lett.* **64**, 1653 (1994).

⁵J. H. Bae, T. Ono, and M. Esashi, *Appl. Phys. Lett.* **82**, 814 (2003).

⁶K.-H. Kim, N. Moldovan, C. Ke, H. D. Espinosa, X. Xiao, J. A. Carlisle, and O. Auciello, *Small* **1**, 866 (2005).

⁷M. Bonnauron, S. Saada, L. Rousseau, G. Lissorgues, C. Mer, and P. Bergonzo, *Diamond Related Materials* **17**, 1399 (2008).

⁸K. Degiampietro and R. Colaco, *Wear* **263**, 1579 (2007).

⁹C. Manfredotti, G. Apostolo, F. Fizzotti, A. Lo Giudice, M. Morando, R. Pignolo, P. Polesello, M. Truccato, E. Vittone, and U. Nastasi, *Diamond Related Materials* **7**, 523 (1998).

¹⁰E.-S. Baik, Y.-J. Baik, and D. Jeon, *Diamond Related Materials* **8**, 2169 (1999).

¹¹Q. Wang, J. J. Li, A. Z. Jin, Z. L. Wang, P. Xu, and C. Z. Gu, *Diamond Related Materials* **15**, 866 (2006).

¹²H. Uetsuka, T. Yamada, and S. Shikata, *Diamond Related Materials* **17**, 728 (2008).

¹³Ph. Niedermann, W. Hanni, D. Morel, A. Perret, N. Skinner, P.-F. Indermuhle, N.-F. de Rooij, and P.-A. Buffat, *Appl. Phys. A: Mater. Sci. Process.* **66**, S31 (1998).

¹⁴D. Alvarez, M. Fouchier, J. Kretz, J. Hartwich, S. Schoemann, and W. Vandervorst, *Microelectron. Eng.* **73–74**, 910 (2004).

¹⁵R. Agrawal, N. Moldovan, and H. D. Espinosa, *J. Appl. Phys.* **106**, 064311 (2009).

¹⁶B. V. Spitsyn, in *Handbook of Crystal Growth*, edited by D. T. J. Hurle, (Elsevier Science, Amsterdam, 1994), Vol. 3.

¹⁷*Handbook of Industrial Diamonds and Diamond Films*, edited by M. A. Prelas, G. Popovich, and L. K. Bigelow (Marcel Dekker, Inc., New York, 1998).

¹⁸*Handbook of Carbon*, edited by H. Pierson (Noyes Publications, Park Ridge, NJ, 1993).

¹⁹J.-K. Lee, M. W. Anderson, F. A. Gray, P. John, J.-Y. Lee, Y.-J. Baik, and K. Y. Eun, *Diamond Related Materials* **13**, 1070 (2004).

²⁰A. V. Khomich, P. I. Perov, V. I. Polyakov, I. G. Teremetskaya, V. P. Varnin, E. D. Obratsova, S. M. Pimenov, and V. G. Balakirev, in *Application of Diamond Films and Related Materials: Third International Conference*, edited by A. Feldman, Y. Tzeng, W. A. Yarbrought, M. Yoshikawa, and M. Murakawa (Government Printing Office, Northwest, 1995), p. 597.

²¹C. Y. Zhang, C. X. Wang, Y. H. Yang, and G. W. Yang, *J. Phys. Chem. B* **108**, 2589 (2004).

²²A. N. Obratsov, A. A. Zolotukhin, A. O. Ustinov, A. P. Volkov, Yu. Svirko, and K. Jefimovs, *Diamond Related Materials* **12**, 917 (2003).

²³X. Wang, K. S. Ryu, D. A. Bullen, J. Zou, H. Zhang, Ch. A. Mirkin, and Ch. Liu, *Langmuir* **19**, 8951 (2003).

²⁴K. H. Kim, R. G. Sanedrin, A. M. Ho, S. W. Lee, N. Moldovan, Ch. A. Mirkin, and H. D. Espinosa, *Adv. Mater.* **20**, 330 (2008).

²⁵D. C. Hurley, M. Kopycinska-Mueller, and A. B. Kos, *J. Miner. Met. Mater. Soc.* **59**, 23 (2007).